Phys. Med. Biol. 45 (2000) 1495–1509. Printed in the UK PII: S0031-9155(00)07527-8

Non-invasive quantitative reconstruction of tissue elasticity using an iterative forward approach

D Fu†, S F Levinson†‡, S M Gracewski§ and K J Parker†

† Department of Electrical and Computer Engineering, University of Rochester, Rochester, NY 14627, USA
‡ Department of Physical Medicine and Rehabilitation, University of Rochester, Rochester, NY 14627, USA
§ Department of Mechanical Engineering, University of Rochester, Rochester, NY 14627, USA

Received 7 September 1999, in final form 4 January 2000

Abstract. A novel iterative approach is presented to estimate Young's modulus in homogeneous soft tissues using vibration sonoelastography. A low-frequency (below 100 Hz) external vibration is applied and three or more consecutive frames of B-scan image data are recorded. The internal vibrational motion of the soft tissue structures is calculated from 2D displacements between pairs

Methods involving static tissue compression have received particular attention of late due to their inherent simplicity. Commonly, the issue of elastic reconstruction is side-stepped by assuming that variations in tissue strain are qualitatively representative of variations in elastic properties. This approach has been used successfully to image relative elastic properties in the detection of otherwise isoechoic lesions in both tissue-mimicking phantoms and in human tissues (Ophir *et al* 1991, 1997, O'Donnell *et al* 1994, Skovoroda *et al* 1995). The primary disadvantage is that artefacts often result because strain is not uniquely determined by variations in Young's modulus, but also by tissue geometry and the distribution of applied forces.

Quantitative reconstruction of soft tissue viscoelastic properties remains the most problematic aspect of virtually all methods of elastography. Skovoroda *et al* (1995) presented a general approach to elastic reconstruction for a linear, elastic, isotropic, incompressible medium subjected to external static compression, based on a plane strain model and known boundary conditions. Skovoroda *et al* (1999) also investigated the problem for large deformations, in which nonlinear displacement–strain relations with high-order spatial derivatives are used. Kallel and Bertrand (1996) developed a regularized linear perturbation approach based on a finite element model and Tikhonov regularization theory. Sumi (1995) proposed a solution to the inverse problem based on a plane stress model from which two-dimensional equilibrium equations are derived, and the spatial distribution of the relative shear modulus is obtained by integration. Romano *et al* (1998) presented the theory and a numerical simulation for non-invasive determination of the material parameter ratios for isotropic, linear elastic media subjected to harmonic vibration.

In this paper, we present a novel iterative forward approach to quantitative estimation of Young's modulus in vibration sonoelastography. In our implementation, three or more consecutive frames of B-scan data are recorded. The two-dimensional displacements between each pair of consecutive frames are estimated using a mesh-based speckle tracking method in which only estimates obtained from nodes with a high feature energy are used, minimizing the risk of speckle decorrelation. The amplitude and phase of the vibration motion vectors are calculated from the estimated displacements. Elastic property reconstruction is formulated as a forward problem based on finite element theory in which an arbitrary region of interest (ROI) is chosen for which Young's modulus, Poisson's ratio and the damping coefficient (viscosity) are assumed to be constant. Given the measured amplitude and phase values of displacement along the boundary of the ROI, the motion vectors for the internal nodes can be calculated from finite element theory based on assumed values of the viscoelastic parameters. An error estimate, calculated from the sum-squared difference (ssd) between the predicted motions and the measured data, is then used to refine the estimate of one or more of these parameters and the

where σ_{ij} is the stress tensor, f_i is the body force vector, u_i is the displacement vector in Cartesian coordinates x_i, ρ is the mass density of the medium; commas in the subscript denote partial differentiation with respect to the indices that follow and summation over repeated indices is implied.

If the material is assumed to be linear, homogeneous, isotropic and viscoelastic, the Voigt

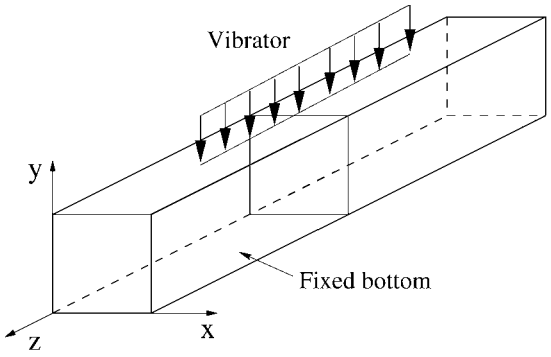

Figure 1. Mechanical model in which a cross section near the middle of the object approximates a plane strain state.

where [m], [c] and [k] are the element mass, damping and stiffness matrices respectively, and {r} are the element grid displacement and force vectors respectively, ω is the angular frequency of vibration and i is the imaginary unit. The [m], [c] and [k] matrices depend on ρ, (λ

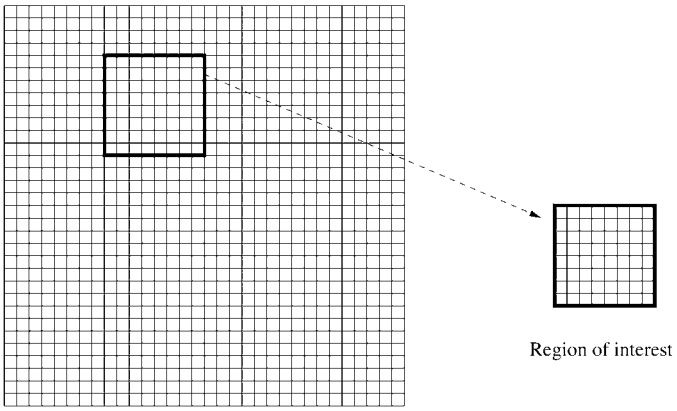

Figure 2. 2D mesh representation of a cross section in which the block shown is an arbitrary region of interest (ROI) within which the mechanical properties are assumed to be constant.

use $\nu = 0.495$, and will explore the validity of this assumption using a numerical simulation in the next section.

Unfortunately, only limited data are available on the viscosity of soft tissues. Based on our own measurements of stress/strain relationships in soft tissue phantoms, we have chosen to ignore damping for the time being. Under conditions where ωC is very small compared with $-\omega^2 M + K$, damping can indeed be ignored and equation (9) can be simpli ed to

[−ø tte162.7(alon)]T/F/F1 1 Tf 855404 0 T[1Fe8)es.3 139(De nmpine)]TJ /F4 1 T6.576433 0 TD'!([)T

Ø tismime9ion8reimatiandYsoduluohe ω K

2.3. Estimation of amplitude and phase

Solving for Young's modulus using the iterative forward approach requires complete 2D vibration amplitude and phase vector field information. Yeung *et al* (1998) developed a mesh-based speckle tracking method based on approaches that are often used in video coding, but adapted for ultrasonic motion tracking. The method employs an adaptive deformable mesh that makes use of image feature energy for assignment of mesh nodes. Ultrasonic speckle results from the constructive and destructive interference of coherent acoustic waves impinging on

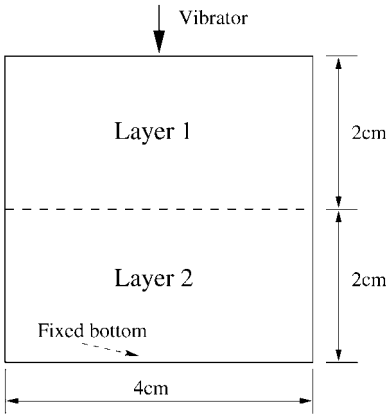

Figure 3.

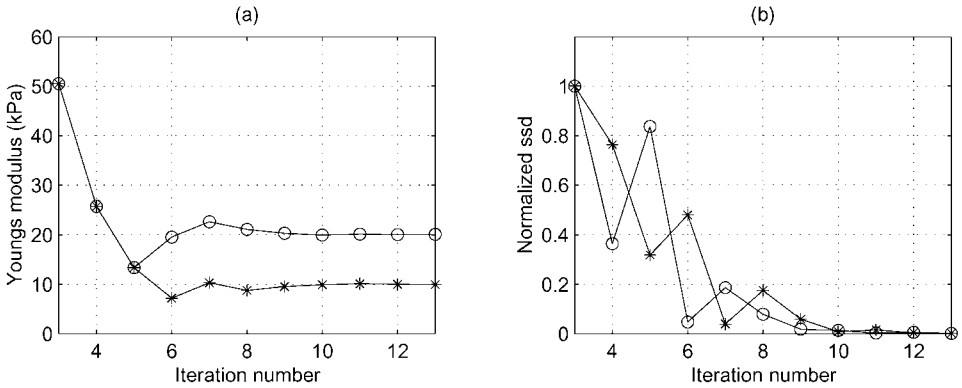

Figure 4. Convergence of results from FEM simulation data. The curves marked □ and ○ represent the soft and hard layers, respectively. (a) Convergence of Young's modulus. (b) Convergence of normalized ssd.

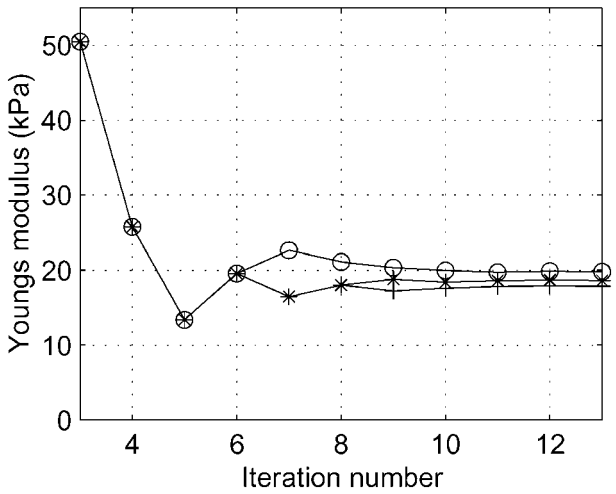

Figure 5. Sensitivity of Young's modulus to errors in the assumed Poisson's ratio for differing sizes of the ROI. The curves marked □, + and ○ represent sizes of the ROI of 6 mm × 6 mm, 8 mm × 8 mm and 10 mm × 10 mm respectively.

different sizes of the ROI (6 mm × 6 mm, 8 mm × 8 mm and 10 mm × 10 mm). The estimation errors were 10.4%, 6.5% and 0.7% respectively, indicating increasing errors as the size of the ROI decreases(m)]TJ,

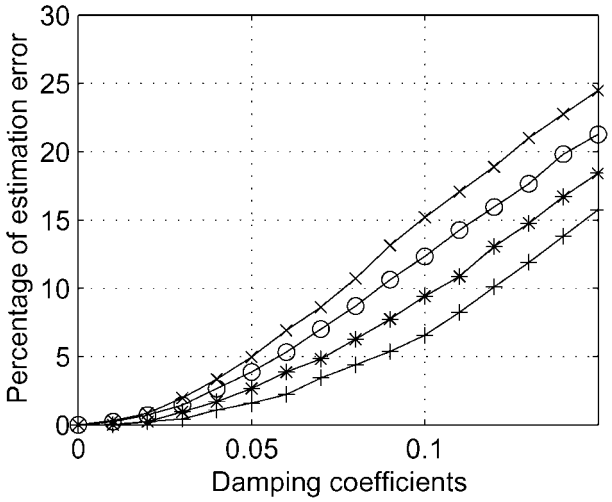

Figure 6. Sensitivity of Young's modulus to damping coef cients at different vibration frequencies. The size of the ROI is 10 mm× 10 mm. The curves marked +, ○ and × represent vibration frequencies of 22.5 Hz, 37.5 Hz, 52.5 Hz and 67.5 Hz respectively.

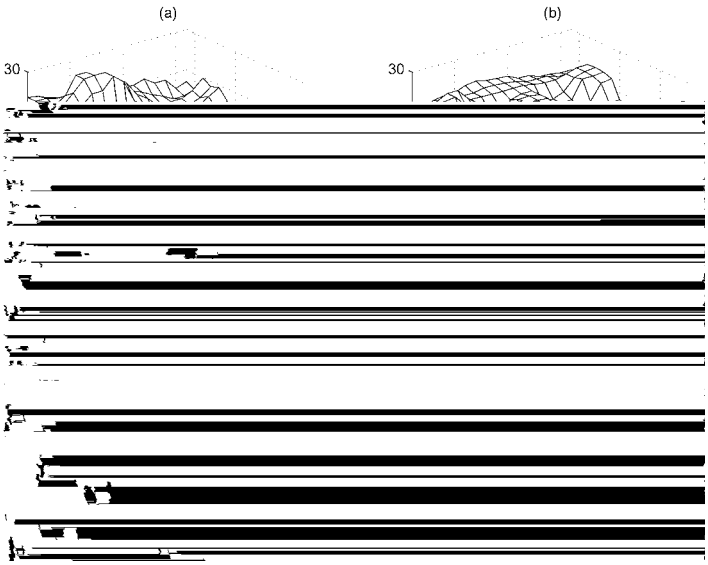

Figure 7. Distribution of Young's modulus in a two-layer structure estimated from simulated noisy displacements where the mean of Gaussian noise is 5% of the maximum displacement at vibration frequencies (a) 22.5 Hz, (b) 37.5 Hz, (c) 52.5 Hz and (d) 67.5 Hz.

noise was arbitrarily chosen to be 5% of the maximum displacement. A complete map of the Young's modulus was obtained by sliding a 10 mm× 10 mm ROI over the entire 2D domain. All of the results were smoothed using a median lter to remove spurious data points. It is noted that the noise performance improved with increasing vibration frequency in regions located entirely within a homogeneous layer. Because Young's modulus is related to the spatial derivatives of the underlying motion, increasing frequencies under conditions

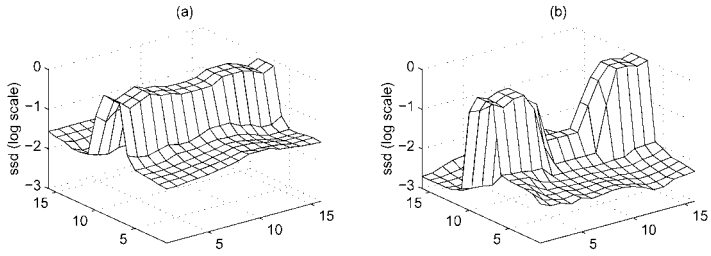

Figure 8. Distribution of log normalized ssd at vibration frequencies (a) 52.5 Hz and (b) 67.5 Hz, corresponding to the distribution of Young's modulus in figures 7(c) and (d) respectively.

of constant amplitude would be expected to result in an improved signal-to-noise ratio, as demonstrated by the results.

From figure 7, it is apparent at the higher vibration frequencies that, when the ROI is located within a homogeneous region, the estimated values of Young's modulus are accurate and stable. However, when the ROI crosses the boundary between two layers, the basic assumption that Young's modulus is constant within the ROI is violated and, hence, the results are unreliable. A confidence measurement can be established by observing the values of ssd. Figure 8 shows the distribution of the normalized ssd on a logarithmic scale. It is apparent that the ssd for regions where the assumption of homogeneity is violated is much larger than in homogeneous regions. It is also noted that the ssd decreases with increasing vibration frequency, suggesting a greater degree of confidence in the estimates obtained.

4. Experiments on tissue-mimicking phantoms

In our approach, reconstruction of the elastic properties of soft tissues involves the use of a mesh-based speckle tracking method to measure the vibrational motion from a B-scan image sequence. Young's modulus is then calculated from the measured vibrational motion using an

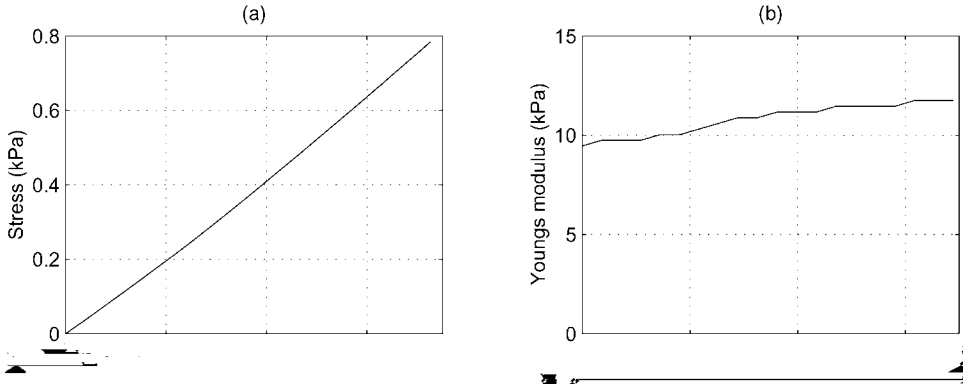

Figure 11. Results from static stress–strain measurements of a small circular cylindrical sample of the material used to construct the homogeneous phantom. (a) Stress–strain data. (b) Calculated Young's modulus.

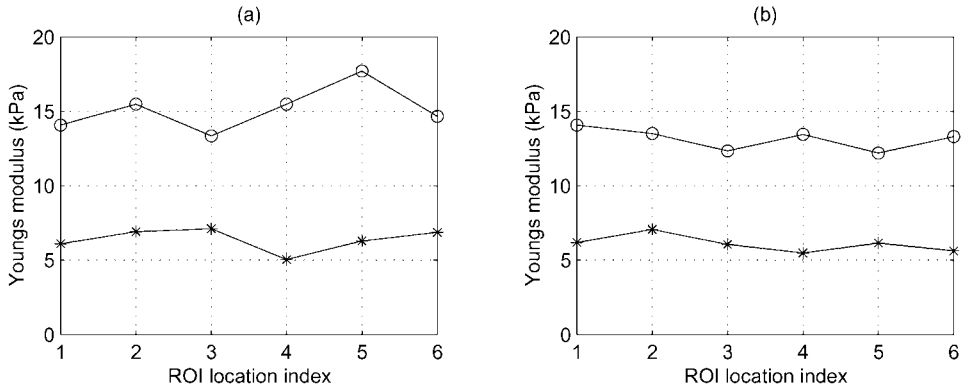

Figure 12. Young's modulus in each of the layers of a two-layer phantom, estimated from ultrasound experiments at vibration frequencies of (a) 67.5 Hz and (b) 97.5 Hz.

modulus values in gure 11(b) were calculated from the slope of the plot of stress versus strain in gure 11(a

Gao L, Parker K J, Alam S K and Lerner R M 1995 Sonoelasticity imaging: theory and experimental veri cation J. Acoust. Soc. Am. 97 3875–86

Hein I A and O'Brien W D 1993 Current time-domain methods for assessing tissue motion by analysis from re ected ultrasound echoes—a review IEEE Trans. Ultrason. Ferroelectr. Freq. Control 40 84–102

Kallel F and Bertrand M 1996 Tissue elasticity reconstruction using linear perturbation method IEEE Trans. Med. Imaging 15 299–313

Kallel F, Bertrand M and Meunier J 1994 Speckle motion artifact under tissue rotation IEEE Trans. Ultrason. Ferroelectr. Freq. Control 41 105–22

Krouskop T A, Dougherty D R and Levinson S F 1987 A pulsed Doppler ultrasonic system for making non-invasive measurements of the mechanical properties of soft tissue J. Rehabil. Res. Dev. 24 1–8

Krouskop T A, Wheeler T M, Kallel F, Garra B S and Hall T 1998 Elastic modulus of breast and prostate tissues under compression Ultrason. Imaging 20 260–74

Lerner R M, Huang S R and Parker K J 1990 Sonoelasticity images derived from ultrasound signals in mechanically vibrated tissues Ultrasound Med. Biol. 16 231–9

Levinson S F, Shinagawa M and Sato T 1995 Sonoelastic determination of human skeletal muscle elasticity J. Biomech. 28 1145–54

Maurice R L and Bertrand M 1999 Speckle-motion artifact under tissue shearing IEEE Trans. Ultrason. Ferroelectr. Freq. Control 46 584–94

Muthupillai R, Lomas D J, Rossman P J, Greenleaf J F, Manduca A and Ehman L 1995 Magnetic resonance elastography by direct visualization of propagating acoustic strain waves Science 269 1854–7

O'Donnell M, Skovoroda A R, Shapo B M and Emelianov S Y 1994 Internal displacement and strain imaging using ultrasonic speckle tracking IEEE Trans. Ultrason. Ferroelectr. Freq. Control 41 314–25

Ophir J, Cespedes I, Ponnekanti H, Yazdi Y and Li X 1991 Elastography: a quantitative method for imaging the elasticity of biological tissues Ultrason. Imaging 13 111–34

Ophir J, Kallel F, Varghese T, Bertrand M, Cespedes I and Ponnekanti H 1997 Elastography: a systems approach J. Imaging Syst. Technol. 8 89–103

Parker K J, Fu D, Gracewski S M, Yeung F and Levinson S F 1998 Vibration sonoelastography and the detectability of lesions Ultrasound Med. Biol. 24 1437–47

Parker K J, Huang S R and Lerner R M 1990 Tissue response to mechanical vibrations for sonoelasticity imaging Ultrasound Med. Biol. 16 241–6

Radmacher M 1997 Measuring the elastic properties of biological samples with the AFM IEEE Eng. Med. Biol. 16 47–57

Romano A J, Shirron J J and Bucaro J A 1998 On the noninvasive determination of material parameters from knowledge of elastic displacements: theory and numerical simulation IEEE Trans. Ultrason. Ferroelectr. Freq. Control 45 751–9

Skovoroda A R, Emelianov S Y and O'Donnell M 1995 Tissue elasticity reconstruction based on ultrasonic displacement and strain images IEEE Trans. Ultrason. Ferroelectr. Freq. Control 42 747–65

Skovoroda A R, Lubinski M A, Emelianov S Y and O'Donnell M 1999 Reconstructive elasticity imaging for large deformation IEEE Trans. Ultrason. Ferroelectr. Freq. Control 46 523–35

Sumi C, Suzuki A and Nakayama K 1995 Estimation of shear modulus distribution of soft tissue from strain distribution IEEE Trans. Biomed. Eng. 42 193–202

Yamakoshi Y, Sato J and -215.8(J)-21k9i.7(and)-215.8(-28r)-158.1(and)-215.8(-28r)-158.1(and)-21